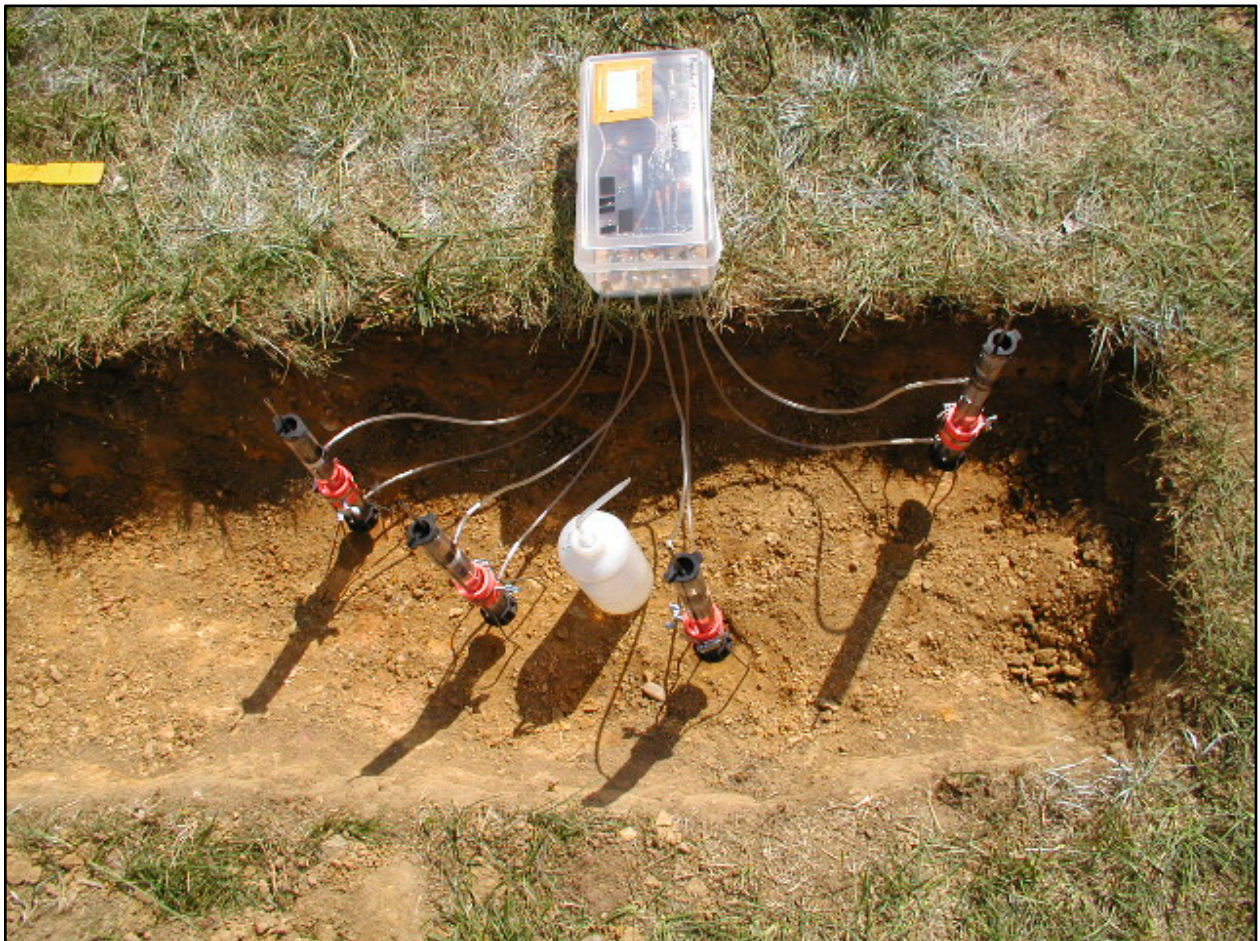


Center for Urban Environmental Research and Education
University of Maryland, Baltimore County

Determining Values of Soil Hydraulic Conductivity in and Around the Gwynns Falls Watershed Using Automated Mini-disk Tension Infiltrimeters

CUERE Technical Report 2009-001
June 2009

Sarah Poole



Determining Values of Soil Hydraulic Conductivity in and Around the Gwynns Falls Watershed Using Automated Mini-disk Tension Infiltrimeters

CUERE Technical Report 2009-001
June 2009

Sarah Poole

University of Maryland, Baltimore County
Center for Urban Environmental Research and Education
1000 Hilltop Circle, Technology Research Center 102
Baltimore, Maryland 21250

This report is available as a downloadable pdf file from the internet at
<http://www.umbc.edu/cuere/BaltimoreWTB>.

Please cite this publication as:

Poole, S. 2009. Determining Values of Soil Hydraulic Conductivity in and Around the Gwynns Falls Watershed Using an Automated Mini-Disk Tension Infiltrimeter. UMBC/CUERE Technical Report 2009-001. University of Maryland Baltimore County, Center for Urban Environmental Research and Education, Baltimore, MD.

ON THE COVER

Test set up of infiltrimeter apparatus in soil pit behind CUERE, August 2008. Photograph by Peter Lapa-Lilly.

Table of contents

Acknowledgements	v
Abstract	vi
1. Introduction	1
2. Study Area	1
3. Methods	3
3.1 Infiltrometer Components and Operation	3
3.2 Automation	4
3.3 Infiltrometer Setup	5
3.4 Calibration	6
3.5 Data Collection in the Field	6
3.6 Sampling Design	9
3.7 Data Analysis	9
3.8 Statistics	11
4. Results	11
5. Discussion	15
5.1 Statistics	15
5.2 Data Collection Errors	16
6. Concluding Remarks	18
7. References	19

List of Figures

Figure 1. Study area and points at which measurements were taken	2
Figure 2. Diagram of mini-disk tension infiltrometer	4
Figure 3. Filling the infiltrometer with water	5
Figure 4. Infiltrometer field setup	7
Figure 5. Volume vs. time graph for a measurement	10
Figure 6. Decrease of infiltration rate with increasingly negative tension	12
Figure 7. Kolmogorov Smirnov Test	12
Figure 8. Tension vs. hydraulic conductivity graph for site D56	13
Figure 9. Tension vs. hydraulic conductivity graph for site W38	13
Figure 10. Tension vs. hydraulic conductivity graph for site W4	14
Figure 11. Tension vs. hydraulic conductivity graph for site W42	14
Figure 12. Graph of relative standard deviations of site grouped in five categories	15
Figure 13. Graph of relative standard deviations in each of the five site categories	16
Figure 14. Volume vs. time graph showing increasing volume	17
Figure 15. Measurement showing increasing infiltration rate with increasing tension	18

List of Tables

Table 1. Start and end times for different test lengths	8
---	---

Appendices

A. Wiring Details	20
B. Summary of Sites	23
C. Tension vs. Hydraulic Conductivity Curves	25
D. Site Description and Images	105

Acknowledgements

This material is based upon work supported by the National Science Foundation under a REU supplement to grant EAR-0610009 and by NOAA grant NA07OAR4170518

I would like to thank Peter Lapa-Lilly for assisting with equipment construction and field work, and Dr. Claire Welty for her continuing guidance through all stages of this project.

Additionally, I would like to thank Dr. Jeff Campbell (UMBC, CUERE) for providing electronics expertise and equipment, Phil Larson and Chrissy Runyan (UMBC, CUERE) for aiding with equipment (GPS, drill press) use, and Tracy Kerchkof (UMBC, CUERE) for creating .kml files used in the sampling design.

Abstract

Point values of soil saturated hydraulic conductivity were measured over a 433 km² area in the vicinity of Baltimore, MD during August and September 2008. The measurements were taken within the Gwynns Falls watershed with approximately 1 km between sites, and outside of the Gwynns Falls watershed with approximately 2 km between sites.

Differential pressure transducers were used to automate infiltrometer measurements of saturated hydraulic conductivity, using an adaptation of a design by Madsen and Chandler (2007). The automation allowed multiple simultaneous in-situ measurements, which were used to characterize the mean and standard deviation at a point. Four measurements were taken at each site. The measurements ranged from highly variable to nearly uniform among measurements at a site.

Over the watershed, the saturated hydraulic conductivity varied from 1.1×10^{-4} cm/s to 2.7×10^{-2} cm/s. The geometric mean was 9.3×10^{-4} cm/s, with a standard deviation of 2.6×10^{-4} cm/s. The distribution of values is lognormal, based on the Kolmogorov-Smirnov test.

The saturated hydraulic conductivity values were used in the Gardner equation to determine hydraulic conductivity as a function of tension. The data are intended to be used in coupled groundwater-surface water model of the region that includes unsaturated zone processes. Although it was not the objective of the work, it was observed that saturated hydraulic conductivity tended to be more variable when at less disturbed (forested) sites.

1. Introduction

The purpose of the study was to compile a dataset of soil hydraulic conductivity values for use in a MODFLOW groundwater model of the Gwynns Falls watershed and surrounding domain. To accomplish this goal, a field campaign was planned and conducted over the summer of 2008 to measure values of soil hydraulic conductivity within the Gwynns Falls watershed and the surrounding area. This effort required design and construction of infiltrometer equipment to carry out the desired measurements.

MODFLOW is a modular three-dimensional finite-difference groundwater model (Harbaugh et al. 2000). The model requires soil hydraulic conductivity values for the model domain as input to calculate the Darcy velocity. Soil hydraulic conductivity is the depth of water that drains through the soil per unit time. The higher the hydraulic conductivity, the faster water can pass through the soil. Hydraulic conductivity can vary over many orders of magnitude over short distances because soil is highly heterogeneous.

The infiltrometers measure soil hydraulic conductivity by holding water under tension. The tension is adjustable, and increasing the tension decreases the rate at which water can leave the infiltrometer and enter the soil. When the tension is adjusted over the course of a measurement, a series of paired values of tension and infiltration rate are collected. These values can be used in Wooding's equation to find the saturated hydraulic conductivity. The saturated hydraulic conductivity can be used in the Gardner equation to find the hydraulic conductivity as a function of tension.

This report begins with a short description of the study area. Next, a significant part of the report is dedicated to the methods used to measure soil hydraulic conductivity: the wiring setup to automate the infiltrometers (with specific details in Appendix A), the data collection methods, and the data analysis methods. Then, a summary of results are presented, with the full listing of saturated hydraulic conductivity values and log tension vs. hydraulic conductivity graphs available in Appendices B and C. Results and measurement errors are then discussed, followed by concluding remarks.

2. Study area

The Gwynns Falls watershed is located in western Baltimore County, MD, and western Baltimore City (Figure 1). The watershed encompasses a northwest-southeast gradient of increasing urbanization, and drains into the Chesapeake Bay. The drainage area of the Gwynns Falls is approximately 66.5 square miles. The model domain, the area outside of the Gwynns Falls watershed, is bounded by the Patapsco River on the west and south, the Jones Falls River on the east, and Western Run on the north. The watershed and domain lie primarily in the Piedmont physiographic province with a small portion in the Atlantic coastal plain (Doheny 1999).

Baltimore County's climate is between humid subtropical and humid continental. The area receives about 43 inches of rainfall annually (Doheny 1999), spaced evenly throughout the year. The primary geologic formations of the Gwynns Falls are the Baltimore Gabbro Complex in the southeast and the Lower Pelitic Schist in the northwest. In addition, a significant area of Baltimore Gneiss, surrounded by thin areas of Setters Formation and Cockeysville Marble, is present in the middle part of the

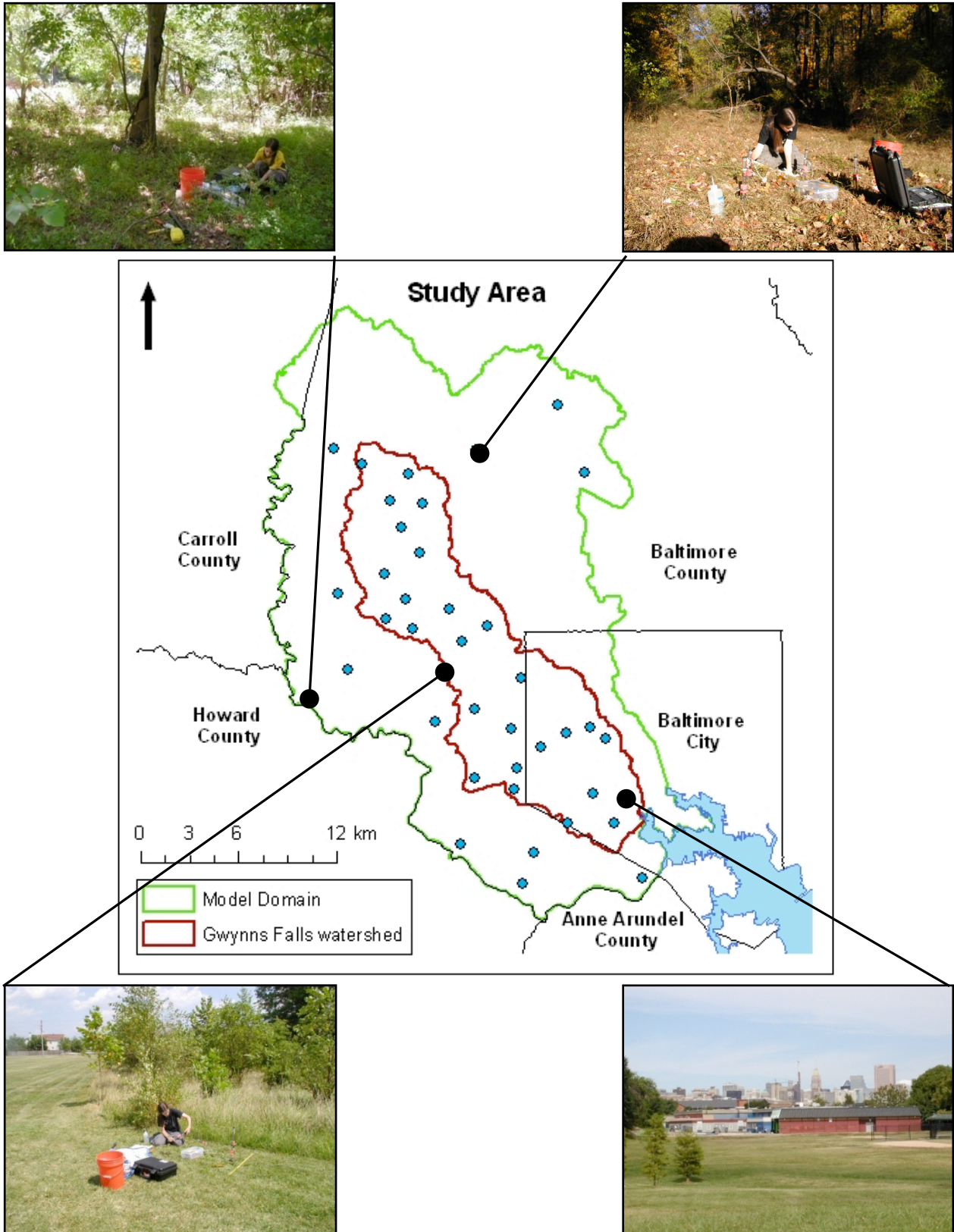


Figure 1. Study area and points at which measurements were taken. Pictures depict urban-suburban-rural (forested) gradient in the study area.

watershed and model domain. The southeastern part of the watershed and domain consists of the Potomac group and lowland deposits. These underlying geologic formations likely are not the parent material of most of the surface soils owing to extensive modification of the landscape from urbanization.

Because it is highly urbanized, the Gwynns Falls watershed contains many urban land and urban-complex soil types. These soils may be brought in from other areas or may be very thin or skeletal. Urban land type soils do not have characteristic hydraulic conductivities or textures listed in soil survey data. New development can cause the soil survey data to become quickly outdated as soil is moved into or out of an area.

Soils in the Gwynns Falls are either young soils (inceptisols), which have very shallow profiles and are not very weathered, or old soils (alfisols), which are highly weathered and have well developed profiles (USDA 1999). The soils typically have a humid (udic) moisture regime and a temperate (mesic) temperature regime (USDA 2007a).

3. Methods

Saturated hydraulic conductivity was measured using an array of four mini-disk tension infiltrometers, following the methodology as outlined by the Young et al. (2007). The infiltrometers are available from Decagon Devices (http://www.decagon.com/geo_civil/hydro/infiltrometer.php), and are not automated by the manufacturer. The infiltrometers were automated by outfitting with differential pressure transducers connected to a data logger. The output voltages from the differential pressure transducers were calibrated to the volume of water that is in the infiltrometer.

3.1 Infiltrometer Components and Operation

The infiltrometer is a narrow clear PVC tube, containing a rubber barrier separating it into two chambers (Figure 2). The top of the infiltrometer contains a stopper with a narrow metal tension selection tube that regulates the amount of suction with which the water is held by the infiltrometer. This tube can be adjusted from -0.5 to -6 cm of suction. The bottom of the infiltrometer is covered by a porous stainless steel disk housed in a rubber base. A Mariotte tube allows the passage of air between the two chambers.

Both chambers are filled with water (Figure 3). When the porous steel disk is placed on the soil surface, water will flow out into the soil. As water flows out of the infiltrometer's base, air flows in through the tension selection tube, bubbles up through the water in the upper chamber, travels down the Mariotte tube, and bubbles up into the lower chamber.

The tension is determined by the depth to which the tension selection tube is below the water surface in the upper chamber. Air must be pulled down through the tension selection tube from outside the infiltrometer against the force of the overlying water.

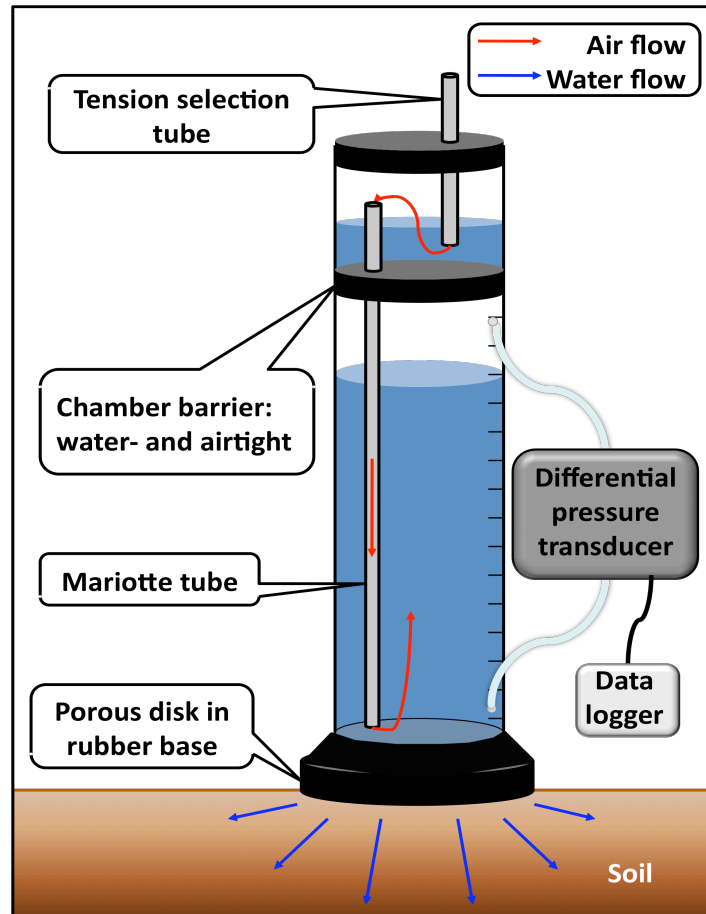


Figure 2 . Diagram of mini-disk tension infiltrometer.

3.2 Automation

Automation of the infiltrometers was accomplished using differential pressure transducers and a data logger. Automation allowed for rapid measurement of water level (every 1 s) and for four simultaneous measurements to be made.

Differential pressure transducers have been used by Casey and Derby (2002) in an attempt to simplify the two transducer set-up used by Ankeny et al. (1988). Ankeny et al. (1988) showed that there is a direct linear relationship between the height of water in the infiltrometer reservoir (the lower chamber) and the pressure in the head space of the reservoir (the space between the rubber chamber barrier and the water). This linear relationship was disrupted by the bubbling that occurs through the water reservoir as the water drains into the soil. Bubbles cause the pressure to increase suddenly in the head space. By using two pressure transducers (or one differential transducer) to sense the difference in pressure between the head space and the bottom of the reservoir where bubbles come out of the bubbling tube, the effect of the bubbles (which cause the same change in pressure at both transducers) is removed through subtraction.



Figure 3. Filling the infiltrometer with water. **A.** First the tubing is connected to the fittings on the infiltrometer (see section 3.3). Then the upper stopper is removed from the infiltrometer, the chamber is filled, the top replaced, and the tension selection tube pushed as far down as possible so that no water will leak out. **B.** The infiltrometer is then inverted, the bottom stopper with the porous disk removed, and filled with water. Trapped air prevents water from entering the tubing during this step. After turning the infiltrometer right side up, the tension selection tube can be set to the desired level for beginning the test.

Madsen and Chandler (2007) automated a tension infiltrometer set up for the purpose of obtaining multiple simultaneous measurements. Simultaneous measurements obtained at one site can be used to compute the mean and standard deviation more quickly than repeating the measurement using a single infiltrometer. A noted disadvantage of this method for obtaining “repeat” measurements is that natural soils are heterogeneous over orders of centimeters. Therefore, these statistics incorporate the effect of microscale soil heterogeneity as well as measurement error. A four-channel data logger is available from HOBO (<http://www.onsetcomp.com/products/data-loggers/u12-006>) and was used to record the output voltages from the pressure transducers.

3.3 Infiltrometer Setup

Using a drill press, two holes were made in each infiltrometer and metal fittings (Pneumadyne, SBF-170) attached to connect 32 mm (1/8 in) tubing to the differential pressure transducers. The upper hole was made near the top of the lower chamber, and the lower hole was made near the bottom of the lower chamber. The metal fittings were inserted into each hole using a power drill. The fittings allowed plastic tubing to easily be connected to and disconnected from the infiltrometer.

The wiring schematic in Madsen and Chandler (2007) was used to design the circuit necessary to connect the data logger to the pressure transducers. Appendix A provides details of the wiring set-up.

3.4 Calibration

Calibration does not need to be done in the lab but rather is a procedure used in the analysis of each measurement. Madsen and Chandler (2007) calibrated each measurement individually because of the variability of voltage output of the transducers throughout the course of a day of measurements, due to changing battery voltage and ambient temperature. The initial and final volumes of water in the infiltrometer were recorded manually in the field, and these were matched with the maximum and minimum output voltages to determine volumes at all points in between, using the equation (Madsen and Chandler 2007):

$$V(t) = V_{\text{tot}}[1 - (v_t - v_{\text{min}}) / (v_{\text{max}} - v_{\text{min}})] \quad (1)$$

where

- V_{tot} = volume of water discharged from the infiltrometer during a measurement; initial volume-final volume (mL)
- v_t = transducer voltage output at time t (volts)
- v_{min} = minimum voltage output for the entire measurement (volts)
- v_{max} = maximum voltage output for the entire measurement (volts)
- $V(t)$ = volume at time t (volts)

Thus, a list of times and corresponding volumes of discharged water was established, similar to the data that would be read manually from the infiltrometer, and was used in the data analysis described below.

3.5 Data Collection in the Field

In the field, each experiment involved using the four infiltrometers operating simultaneously. PVC pipe sections with supporting legs attached by a hose clamp were used to keep the infiltrometers upright during measurement, following a design in Madsen and Chandler (2007). These stands were also used to keep the infiltrometers above the soil surface before the beginning of the experiment. The infiltrometers were spaced 45 cm apart in a semicircle, with the box of wiring in the center (Figure 4).

The infiltrometers were filled with tap water from gallon jugs. Deionized water was not used because of its tendency to disperse soil clays and to change the ionic balance of the soil (Decagon Devices, 2006).

Before the test began, the soil surface where each infiltrometer would be placed was cleared of vegetation and debris using a plastic putty knife (or a pocket knife for vegetation with thicker roots). The soil was then made approximately level so that the infiltrometer would not be tilted.

Temperature of the infiltrating water was measured using a temperature probe before and after each experiment, since saturated hydraulic conductivity depends on temperature. Temperature of the water changed over the course of each experiment, either due to solar heating of the water or fluctuations in air temperature. GPS coordinates were also recorded; however, if the GPS did not work because of tree

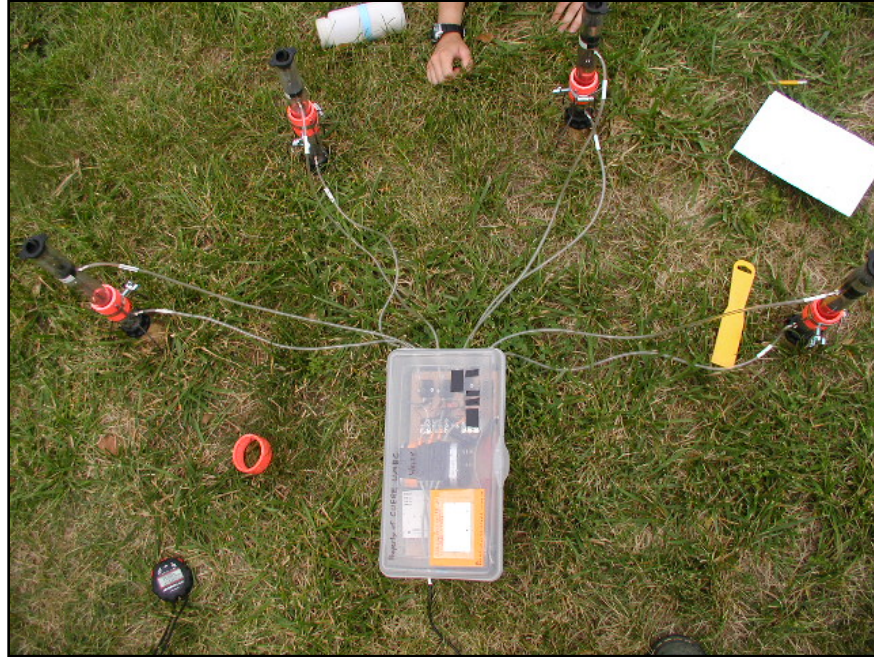


Figure 4. Infiltrometer field setup. Infiltrometers were positioned in a semi-circle, with adjacent infiltrometers 45 cm apart.

or cloud cover, then measurements from landmarks were taken to approximate the location using high-resolution orthoimagery back in the lab. GPS coordinates (or the data file name in which they were stored by the GPS device) and temperature measurements were recorded on a data sheet for each measurement, along with the file name of the data read out by the data logger.

The infiltrometers were set at the lowest tension (least negative) first (Logsdon and Jaynes 1993). The tension steps used were -0.5, -2, -3, -4, and -5 cm.

Three different test lengths were used in this study: 9-minute, 13-minute, and 25.5-minute. The different lengths were used so that enough water would infiltrate to get an accurate measurement but also so that the infiltrometer would not run out of water during the test. At the beginning of each experiment, the pressure transducers were powered for 30 seconds before the first infiltrometer was placed onto the soil surface to eliminate any initial voltage jumps.

The data logger records time, in seconds from the start of its recording, and voltage that it receives from the pressure transducers. A stopwatch was started at the same instant that the data logger began recording. At the times listed in Table 1, the infiltrometers were started, the tensions changed, and the tests were ended. The time and voltage readings of the data logger could then subsequently be linked to the infiltrometer tension at the correct time. For example, in a 13-minute test, the data recorded for infiltrometer 1 between 3:00 and 5:30 were during the time when the infiltrometer was set at a tension of -2 cm, and were used in data analysis to calculate the infiltration rate at -2 cm.

Because the four infiltrometers all needed to be started, adjusted, and stopped at an exact time, staggered times were used, since all infiltrometers could not be started, adjusted or stopped

simultaneously. Fifteen-second gaps gave sufficient time to lower one infiltrometer to start the test and assure good contact with the soil before moving on to start the next infiltrometer.

Note: the 9-minute test only allows 30 seconds for each infiltrometer at the initial tension, thus resulting in time conflicts between starting infiltrometer 3 and adjusting infiltrometer 1 to a higher tension. This test was only done in a few circumstances when the infiltrometers would almost completely drain during the 2.5 minute period at -0.5 cm tension. It was necessary to have two people at the beginning of the test: one to start all of the infiltrometers and one to adjust the tensions.

Prior to the four-infiltrometer experiment at each site, an initial manual test was conducted to quickly assess the approximate infiltration rate of the soil, which determined the run length required for the four-infiltrometer automated experiment. If the infiltration was less than 10 mL in 13 minutes, a 25.5-minute test was run. If the infiltration was more than 10 mL, a 13-minute test was run. In addition, a 9-minute test, allowing for thirty seconds at -0.5 cm tension and 2 minutes at each subsequent tension, was occasionally run if the infiltration was very fast and the infiltrometers ran out of water during the 13-minute test.

Table 1. Start and end times for different infiltrometer test lengths.

Event	Infiltrometer	9 minute test	13 minute test	25.5 minute test
Start test (at -0.5 cm tension)	1	0:30	0:30	0:30
	2	0:45	0:45	0:45
	3	1:00	1:00	1:00
	4	1:15	1:15	1:15
Adjust -0.5 cm → -2 cm tension	1	1:00	3:00	5:30
	2	1:15	3:15	5:45
	3	1:30	3:30	6:00
	4	1:45	3:45	6:15
Adjust -2 cm → -3 cm tension	1	3:00	5:30	10:30
	2	3:15	5:45	10:45
	3	3:30	6:00	11:00
	4	3:45	6:15	11:15
Adjust -3 cm → -4 cm tension	1	5:00	8:00	15:30
	2	5:15	8:15	15:45
	3	5:30	8:30	16:00
	4	5:45	8:45	16:15
Adjust -4 cm → -5 cm tension	1	7:00	10:30	20:30
	2	7:15	10:45	20:45
	3	7:30	11:00	21:00
	4	7:45	11:00	21:15
End test	1	9:00	13:00	25:30
	2	9:15	13:15	25:45
	3	9:30	13:30	26:00
	4	9:45	13:45	26:15

The initial test was done because the pressure transducer data are often erroneous when the volume of water in the infiltrometer does not change very much. A longer test allowed for more water to infiltrate, generating more accurate data. A shorter test for quick infiltration was used so that the infiltrometer did not become completely empty during the course of the test.

The logger was connected to a laptop in the field. The data were downloaded from the logger onto the laptop immediately after the measurement was complete.

3.6 Sampling Design

Measurements of saturated hydraulic conductivity were taken within the Gwynns Falls watershed as well as within the larger groundwater model domain for the MODFLOW model of interest.

In order to determine the sampling grid, first a regular grid with 0.5 km/side grid squares was overlaid on the watershed and domain. Spacing the saturated hydraulic conductivity measurements out over 2 km/side grid squares within the watershed and 4 km/side grid squares in the domain gave reasonable spatial coverage within the timeframe available in which to conduct the fieldwork. This resulted in sixty-six measurement points, 42 within the Gwynns Falls watershed and 24 in the larger model domain outside of the Gwynns Falls watershed boundary.

An overlay of Baltimore City and County public lands and roads was used to find the closest available sampling site to the grid data points. Sampling sites were labeled, and information about accessing the site and alternate sites if access was not possible was also recorded.

3.7 Data Analysis

The data collected in the field first had to be transformed into values of $q(h)$, the one dimensional steady state infiltration for each tension (cm/s). To determine $q(h)$ from volume of water recorded in the field at each time, the infiltration rate, I_t (mL/s), was calculated by fitting a linear trendline through the data (volume vs. time) that was collected during each tension step. The slope of the trendline was I_t . The trendline was used because the voltage tended to fluctuate. An example is shown in Figure 5.

The -0.5 cm tension was not used in the calculations because the initial fluctuation as the infiltrometer was placed on the soil surface was typically very high. In addition, the moisture content of the soil was still changing during this tension step instead of being close to saturation like in the successive tension steps.

Data were also ignored for two seconds before and two seconds after the tension was adjusted each time. The sudden increase in tension often caused erroneous voltage readings.

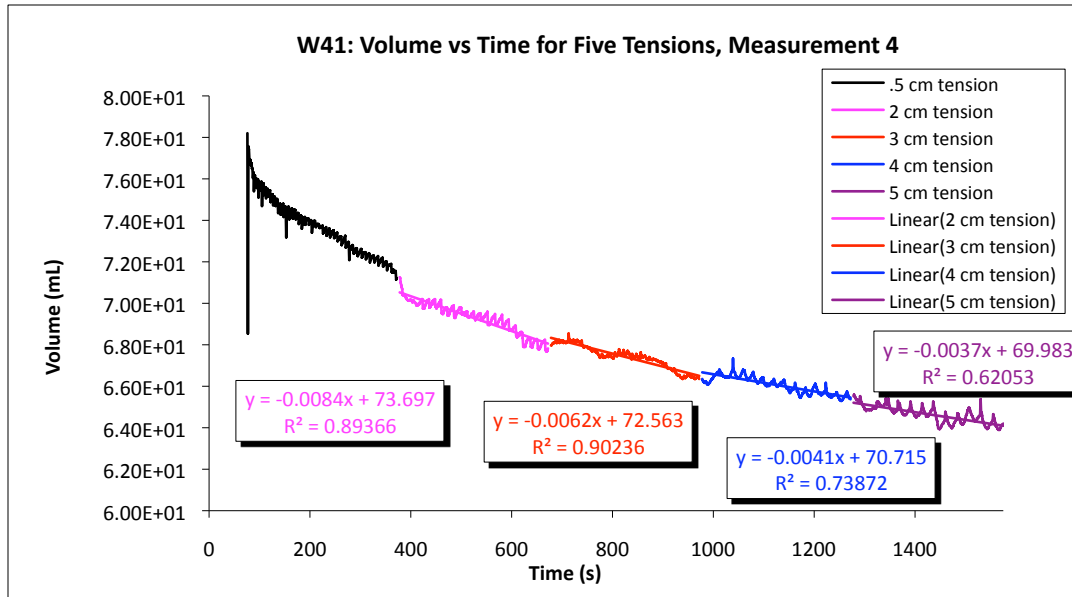


Figure 5. Volume vs. time graph for a measurement. Voltage fluctuations are especially evident in the -4 and -5 cm tensions.

Next, the infiltration rate in mL/s was transformed into cm/s using the formula (Decagon 2006):

$$q(h) = I_t / (\pi r^2) \quad (2)$$

where

- q = one dimensional steady state infiltration rate (cm/s)
- h = tension, selected on the infiltrometer (cm)
- I_t = infiltration rate at time t (mL/s)
- R = radius of infiltrometer disk (cm)

The method for analyzing data in Young et al. (2004) and Young et al. (2007) uses Wooding's equation to find the saturated hydraulic conductivity:

$$q(h) = K_s e^{\alpha h} (1 + (4/\pi r \alpha)) \quad (3)$$

where

- q = one dimensional steady state infiltration rate (cm/s) (from eq. 2)
- h = tension, selected on the infiltrometer (cm)
- K_s = saturated hydraulic conductivity (cm/s, unknown)
- α = pore size distribution parameter (cm^{-1} , unknown)
- r = radius of infiltrometer's disk (cm)

A range of tensions and corresponding infiltration values were known from the field data. These were inserted into the equation and nonlinear least squares regression (an exponential trendline) was used to solve for the two unknown variables α (pore size distribution) and K_s . This method uses only the steady

state infiltration rates to determine K_s . The exponential trend line, $y=ce^{bx}$ is used, where $y=q(h)$, $x=h$, $c=K_s(1+(4/\pi r\alpha))$ and $b=\alpha$. Values of the coefficients c and b are found using the trendline equation.

The K_s value is corrected for temperature of infiltrating water according to the following formula (Young et al. 2007):

$$K_s^{20C}=K_s(1.498e^{-T/28.8}+0.269) \quad (4)$$

where

K_s^{20C} = saturated hydraulic conductivity corrected to a temperature of 20°C (cm/s)

K_s = saturated hydraulic conductivity found by the previous equation (cm/s)

T = measured water temperature °C

The K_s value can then be used as model input. Once the K_s and α are known, they can be used in the Gardner Equation (Young et al. 2007):

$$K(h)=K_s e^{\alpha h} \quad (5)$$

where

$K(h)$ = hydraulic conductivity as a function of tension (cm/s)

From this equation, tension vs. hydraulic conductivity curves were generated. These curves were plotted on logarithmic axes so that a wide range of values could be displayed.

3.8 Statistics

After the K_s values were calculated for each individual measurement, the geometric mean and standard deviation (the mean and standard deviation of the logarithms) of the four measurements at one site were calculated. The mean K_s for each site was used to compare values across the entire dataset.

The hydraulic conductivity as a function of tension equations were generated for each individual measurement, as well as for the average K_s (\pm standard deviation) at each site. These functions were plotted using Excel to show log tension (absolute value of the negative tension) vs. hydraulic conductivity.

4. Results

Measurements were made at forty out of the sixty-six planned sites. Spatial coverage of the watershed was reasonable with this number of measurements; however, in the eastern part of the model domain, measurement density was somewhat lower than in the rest of the study area (Figure 1).

A typical measurement showed a decrease in infiltration rate with increased tension (Figure 6). The coefficients from the fitted exponential line could then be used in Wooding's equation.

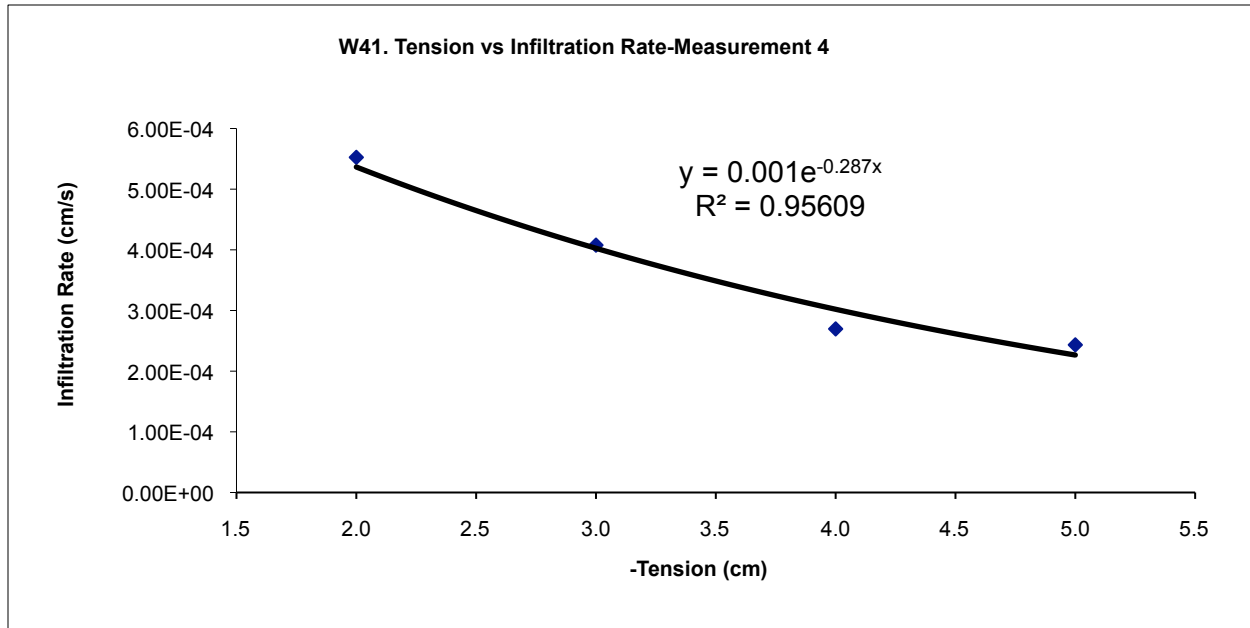


Figure 6. Decrease of infiltration rate with increasingly negative tension.

The mean values of K_s for each site (mean of four infiltrometer measurements) were used in the Kolmogorov-Smirnov test (Figure 7) and were found to be lognormal. As hydraulic conductivity increased, the standard deviation tended to increase, so a relative standard deviation was determined for comparison of variability at different sites. The relative standard deviation is defined as the standard deviation divided by the mean.

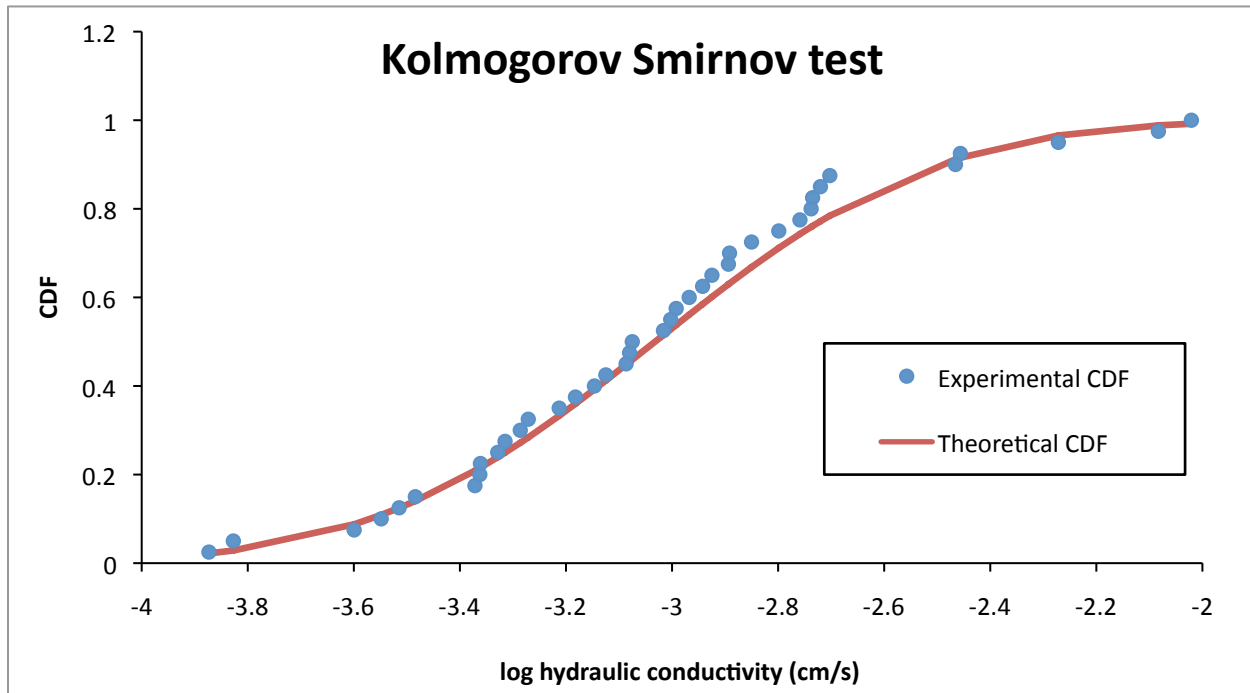


Figure 7. Kolmogorov Smirnov test for lognormality.

Tension vs. hydraulic conductivity curves exhibited a variety of patterns. Examples are shown in Figures 8, 9, 10, and 11. Deviation did not always increase with hydraulic conductivity; at some sites, despite high conductivity, there was little deviation. At other sites, a moderate mean conductivity contained considerable deviation.

Appendix B contains a listing of saturated hydraulic conductivity values, and Appendix C contains a complete listing of hydraulic conductivity as a function of tension equations and graphs.

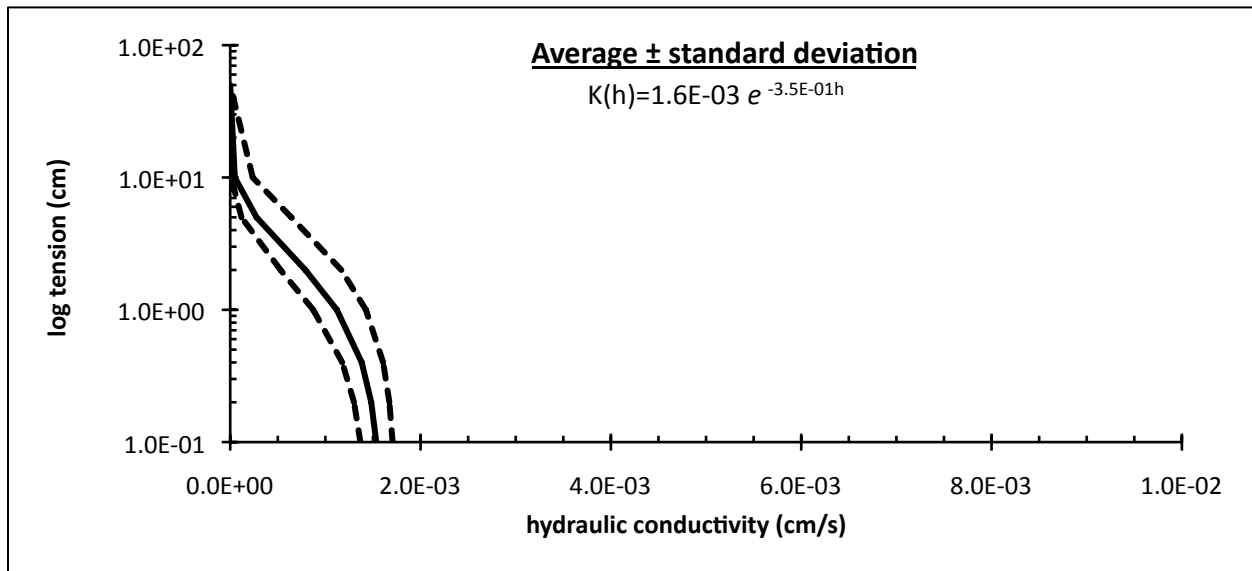


Figure 8. Tension vs. hydraulic conductivity graph for site D56. Liberty Rd at Lyons Mill Rd. At this site, hydraulic conductivity was moderate (1.6×10^{-3} cm/s), and standard deviation was low.

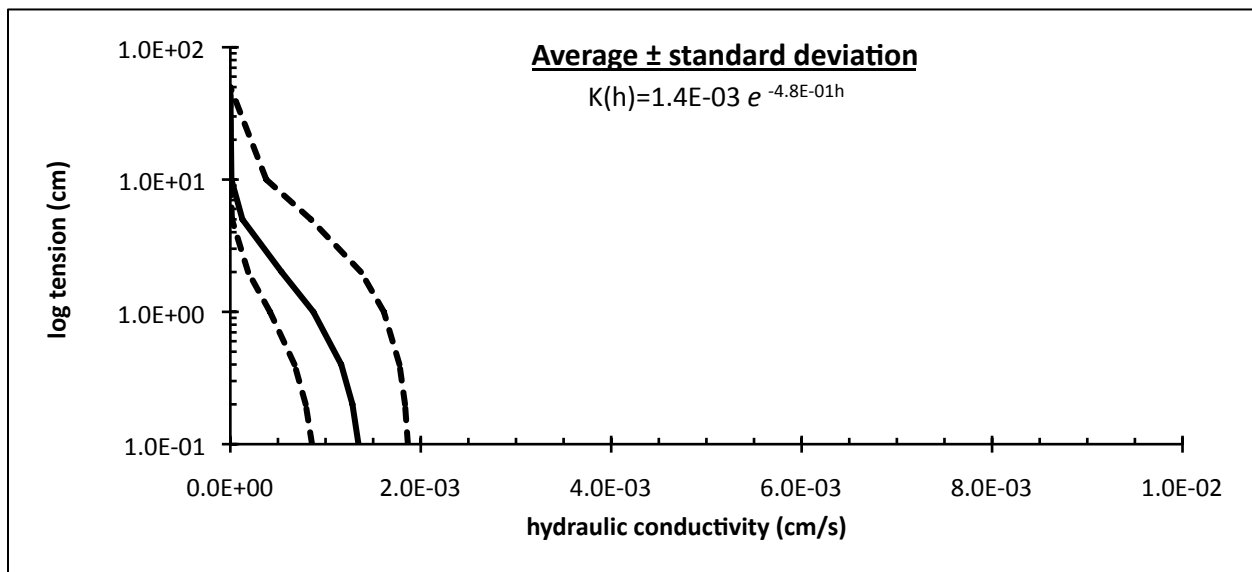


Figure 9. Tension vs. hydraulic conductivity graph for site W38. SWR at Gwynnbrook Ave. Although the hydraulic conductivity is approximately the same as in Figure 8, the standard deviation is considerably higher.

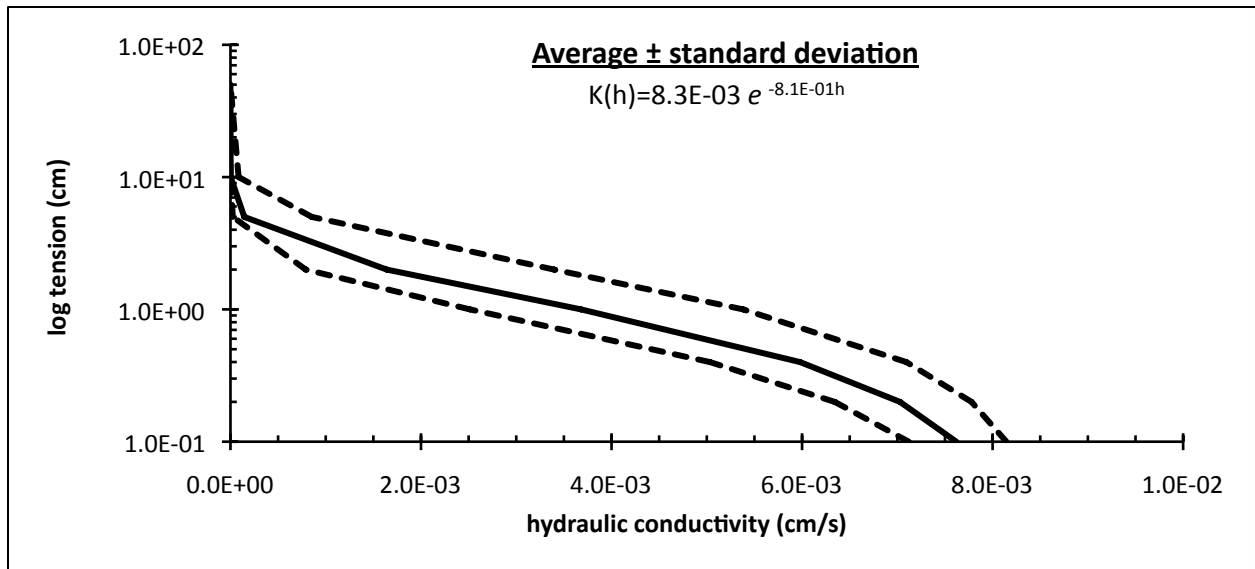


Figure 10. Tension vs. hydraulic conductivity graph for site W4. Southwestern High School. This site had the second highest mean hydraulic conductivity, and had high deviation. However, because the hydraulic conductivity was high, the relative standard deviation was among the lowest of all the sites.

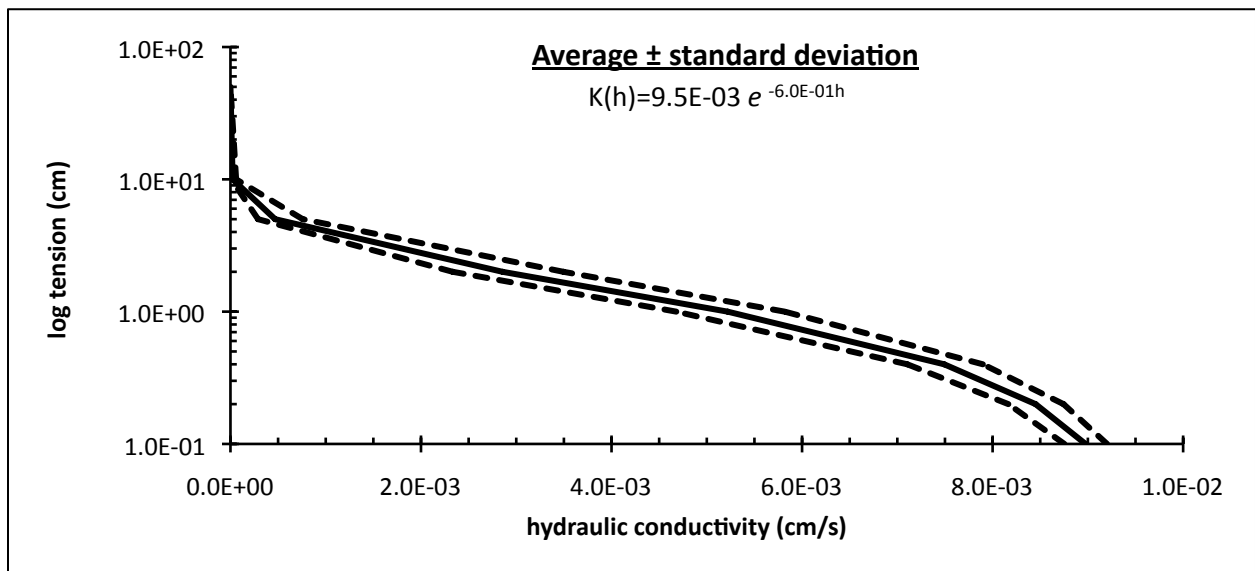


Figure 11. Tension vs. hydraulic conductivity graph for site W42. Chatsworth School. This site had the highest hydraulic conductivity value, and one of the lowest standard deviations. It had the lowest relative standard deviation (1.6%).

5. Discussion

5.1 Statistics

The range of relative standard deviations showed that in a single site, saturated hydraulic conductivity ranged from highly variable (94% relative standard deviation) to uniform (1.6% relative standard deviation).

The most highly variable sites (high relative standard deviation) were forested (Figures 12 and 13). Less variable sites seemed to occur in more altered areas, such as parks and leveled athletic fields. The soil of altered areas is often fill brought in from other areas and homogenized by the bulldozing process. Soils in forested areas are less disturbed and have developed a heterogeneous structure over long periods of time. The soil in areas of woody vegetation contains more large roots and heterogeneity.

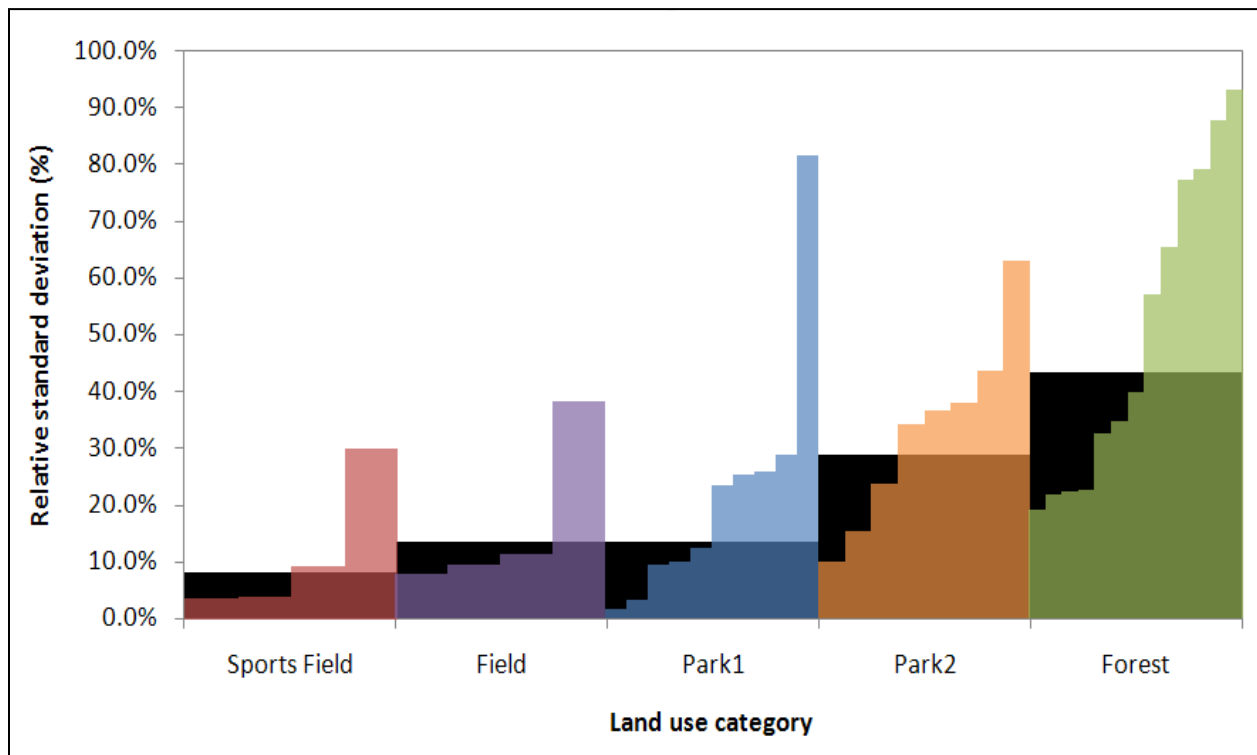


Figure 12. Graph of relative standard deviations of saturated hydraulic conductivity of sites grouped in five categories. Sports field is a mowed grass area that has been leveled. Field is a grassy area with no nearby trees. Park1 is a mowed grass field with some nearby trees. Park2 is a mowed grass area with more nearby trees. Forest is a site with predominantly woody vegetation. Disturbance of sites increases from right to left, and prevalence of woody vegetation increases left to right. The black bars in the background show the geometric mean of all relative standard deviations in that category, and the colored bars in the foreground show each measurement.

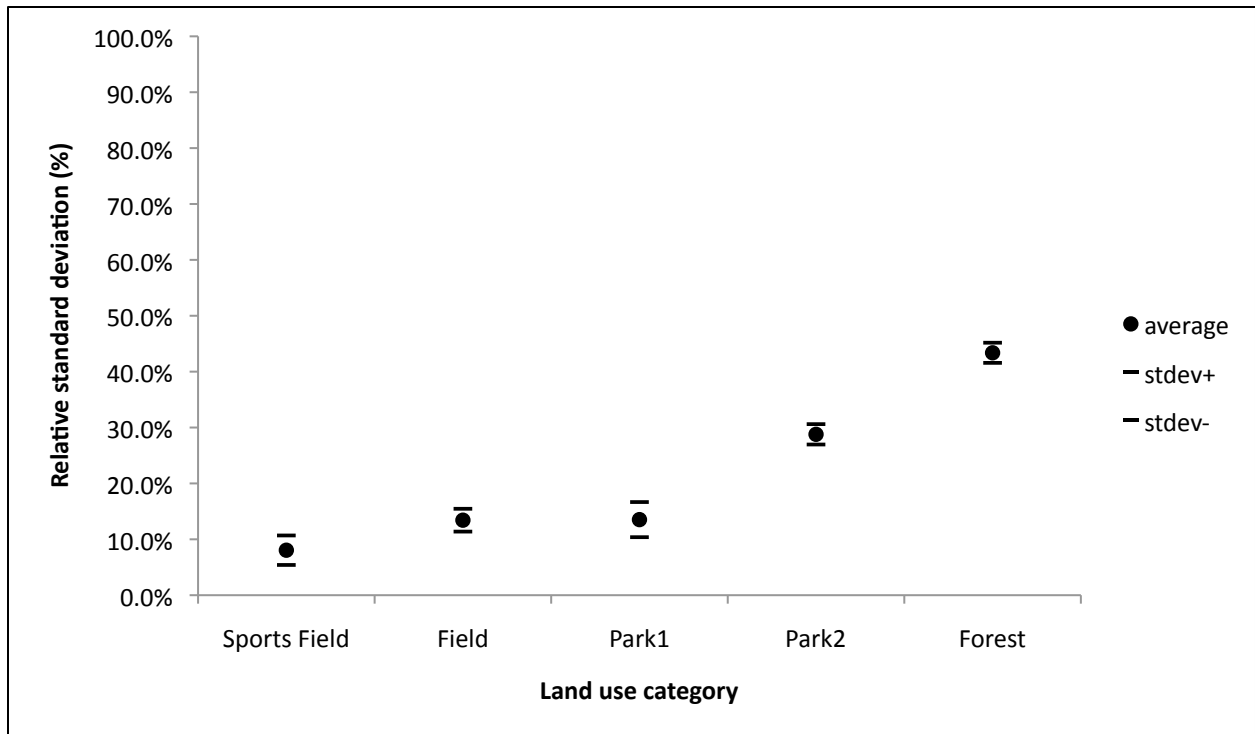


Figure 13. Graph of average and standard deviations of relative standard deviations in each of the five site categories. Sports field is a mowed grass area that has been leveled. Field is a grassy area with no nearby trees. Park1 is a mowed grass field with some nearby trees. Park2 is a mowed grass area with more nearby trees. Forest is a site with predominantly woody vegetation. Disturbance of sites increases from right to left, and prevalence of woody vegetation increases left to right.

5.2 Data collection errors

Errors can be broken down into errors in a single tension and errors in the overall measurement. Errors in a single tension included negative infiltration, extreme voltage jumps/drops, and emptying of water before the end of the test. Errors in a single tension do not make the measurement unusable, but errors in two or more tensions in the same measurement did not allow calculation of saturated hydraulic conductivity, since no trendline could be generated. In addition, the overall measurement could be unusable if the infiltration rate increased with tension, or no trend was observed (very low R2, little or no curve to trendline).

Slow infiltration rates led to negative infiltration errors. The pressure transducers often read an increase in voltage (corresponding to an increase in water level, which is not physically possible) when there was little or no infiltration (Figure 14). Slow infiltration typically happened at the higher (more negative) tensions. As a result, negative infiltration values for these tensions were calculated in the data analysis. These values were unusable in generating the exponential fit line for use in Wooding's equation. The exponential fit line required at least three of the four tensions, so if infiltration was too slow through more than one tension in a measurement, that measurement was unusable in the average and standard deviation calculations. Negative infiltration was responsible for 47% of unusable tensions.

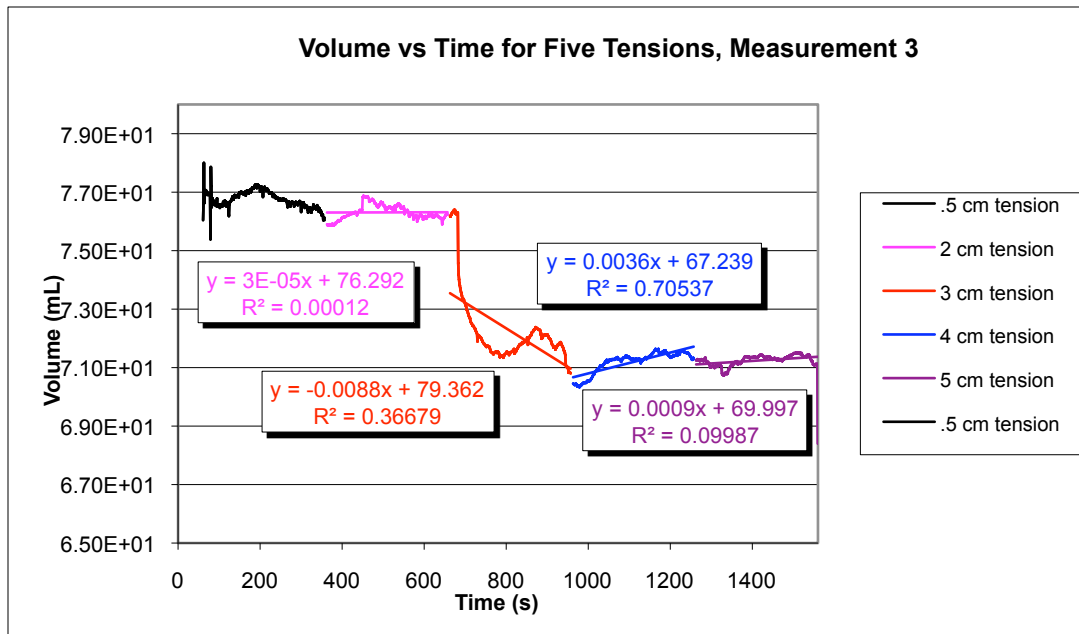


Figure 14. Volume vs. time graph showing increasing volume. The -2, -4 and -5 cm tensions (from 363 s to 637 s and from 963 s to 1560 s) show a negative infiltration rate because they have a positive slope, indicating an increase in water level inside the infiltrometer. The -3 cm tension (from 663 s to 957 s) is also in error. This measurement was unusable in calculating saturated hydraulic conductivity.

Another source of error was due to unexplained voltage jumps or drops, resulting in very high or low values for a single tension in a measurement. These errors were responsible for 41% of unusable tensions. Additionally, 12% of unusable tension steps resulted from the infiltrometer emptying of water before the end of the experiment.

Of measurements that were completely unusable, 30% were due to two or more tension steps having errors, and 40% were due to tensions having no trend between them. In addition, the infiltration rate occasionally increased with tension (Figure 15). Wooding's equation depends on the decrease of infiltration rate with tension, so these measurements were also unusable. This error was not likely the result of a misreading of the pressure transducer, because a similar error had been observed in measurements where the water level was read directly from the infiltrometer. This error was the cause of 30% of unusable measurements.

Voltage errors caused unusable measurements for at least one infiltrometer at 35% of sites visited. One site had only one usable measurement. Approximately 9% of all tension steps were unusable. (The measurement itself may have been usable however, because only 3 of 4 tensions were required to calculate the saturated hydraulic conductivity.)

Most voltage errors could probably be eliminated with better wiring and connections between components. Additionally, it was found that constricting the tubes leading to the pressure transducers tended to reduce voltage fluctuations, so perhaps smaller diameter tubing would give better results. Better control of the temperature of the components may also make measurements more accurate.

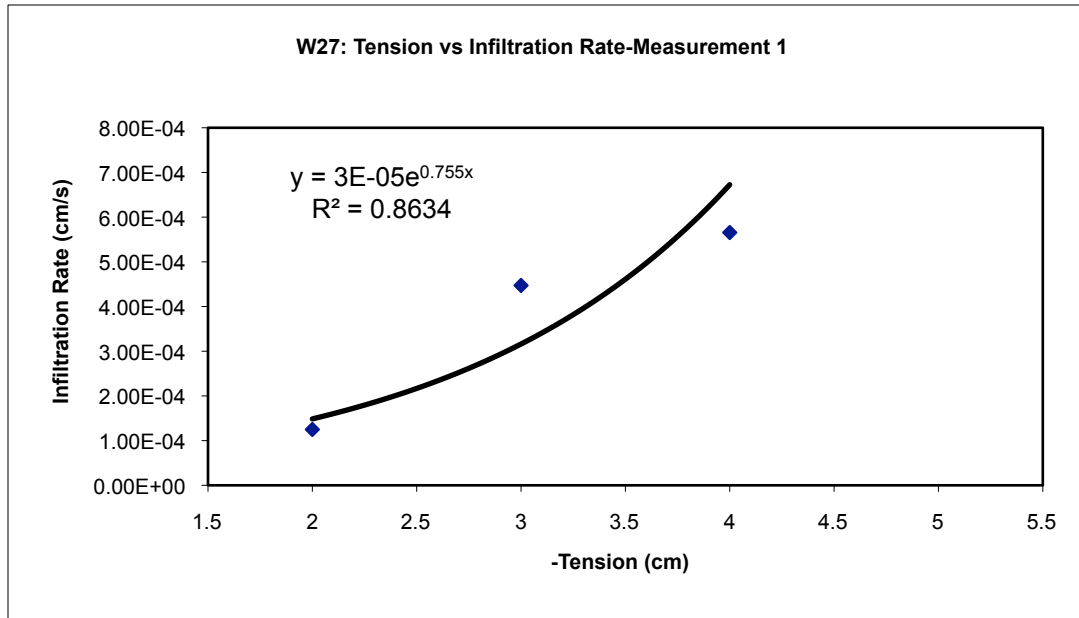


Figure 15. Unusable measurement showing increasing infiltration rate with increasing tension. Because infiltration rate increased with tension, the exponent was positive, meaning that α was negative. A negative α causes a negative saturated hydraulic conductivity, which is not possible.

6. Concluding remarks

Hydraulic conductivity was successfully measured at 40 out of the 66 sites originally planned for this study. The geometric mean of the measurements was 9.3×10^{-4} cm/s, with a geometric standard deviation of 2.6×10^{-4} cm/s. These values are well within the range of typical values of saturated hydraulic conductivity listed in the soil surveys for the region (USDA 2007b). As the mean increased, the standard deviation increased, so the relative standard deviation (standard deviation/mean) was used to compare the sites' variability.

As expected, soil hydraulic conductivity could be highly variable at a small spatial scale (94% relative standard deviation). However, hydraulic conductivity was also very uniform at some sites (1.6% relative standard deviation). Soil heterogeneity seemed to be controlled in part by the variable nature of soil but also in part by the type of vegetation (some types of which more readily obstructed flow of water). More heterogeneous measurements were obtained in less disturbed sites, such as forested sites, whereas more homogenous measurements were obtained in highly disturbed sites, such as leveled athletic fields.

Measurement errors were fairly common and resulted in measurements that were unusable in calculations of saturated hydraulic conductivity. However, enough data were obtained to calculate some basic statistics.

7. References

- Ankeny MD, Kaspar TC, Horton R. 1988. Design for an automated tension infiltrometer. *Soil Sci Soc Am J.* 52(3):893-896.
- Casey FM, Derby NE. 2002. Improved design for an automated tension infiltrometer. *Soil Sci Soc Am J.* 66(1): 64-67.
- Decagon Devices. c2006. Mini disk infiltrometer user's manual (Version 3). Pullman (WA): Decagon Devices, Inc.
- Doheny EJ. 1999. Index of hydrologic characteristics and data resources for the Gwynns Falls watershed, Baltimore County and Baltimore City, Maryland. Baltimore (MD): U.S. Geological Survey. Open-File Report No. 99-213.
- Harbaugh AW, Banta ER, Hill MC, McDonald MG. 2000. MODFLOW-2000, the U.S. Geological Survey modular ground-water model—User guide to modularization concepts and the ground-water flow process. Reston (VA): U.S. Geological Survey. Open-File Report No. 00-92.
- Logsdon SD, Jaynes DB. 1993. Methodology for determining hydraulic conductivity with tension infiltrometers. *Soil Sci Soc Am J.* 57(6): 1426-1431.
- Madsen MD, Chandler DG. 2007. Automation and use of mini disk infiltrometers. *Soil Sci Soc Am J.* 71(5): 1469-1472.
- USDA. 1999. Soil Taxonomy: A basic system of soil classification for making and interpreting soil surveys. Washington (DC): U.S. Government Printing Office. p 163, 489.
- USDA. 2007a. Taxonomic Classification of the Soils: Baltimore County, Maryland.
- USDA. 2007b. Physical Soil Properties: Baltimore County, Maryland.
- Young MH, Caldwell TG, Miller JJ, Dalldorf GK. 2007. Hydraulic characteristics of soil contributing to the Windmill Wash detention basin near Bunkerville, Nevada. Desert Research Institute.
- Young MH, McDonald EV, Caldwell TG, Benner SG, Meadows DG. 2004. Hydraulic properties of a desert soil chronosequence in the Mojave Desert, USA. *Vadose Zone J.* 3(3): 956-963.